J|A|C|S
COMMUNICATIONS

Published on Web 03/11/2008

# Two-Photon Fluorescent Turn-On Probe for Lipid Rafts in Live Cell and Tissue

Hwan Myung Kim,[†] Byeong Ha Jeong,[‡,§] Ju-Yong Hyon,[||] Myoung Jin An,[†] Mun Sik Seo,[†] Jin Hee Hong,[‡,§] Kyoung J. Lee,[‡,§] Chul Hoon Kim,[⊥] Taiha Joo,[⊥] Seok-Cheol Hong,*[,§] and Bong Rae Cho*[,†]

*Department of Chemistry, National Creative Research Initiative Center for Cell Dynamics, Department of Physics, Biomicrosystems Technology Program, Korea University, 1-Anamdong, Seoul, 136-701, Korea, and Department of Chemistry, Pohang University of Science and Technology, Pohang, 790-784, Korea*

Received January 1, 2008; E-mail: hongsc@korea.ac.kr; chobr@korea.ac.kr.

**Ⓦ This paper contains enhanced objects available on the Internet at http://pubs.acs.org/journals/jacsat.**

The lipid rafts hypothesis claims that plasma membrane has rigid compartments [liquid-ordered ($l_o$) phase] enriched with glycosphingolipids and cholesterol floating in the sea of glycerophospholipids [liquid-disordered ($l_d$) phase].[1−5] The rigid compartments, also called rafts, are believed to be involved in many cellular processes such as signal transduction, pathogen invasion, cholesterol homeostasis, neurodegenerative diseases, and angiogenesis.[1−5] To understand their roles in biology, it is crucial to visualize such domains in living cells and tissues. An ideal tool for that purpose is two-photon microscopy (TPM) that uses two near-infrared photons for excitation.[6,7] We recently reported a useful TP polarity probe for the lipid rafts, 6-dodecanoyl-2-[*N*-methyl-*N*-(carboxymethyl)amino]naphthalene (CL), which is superior to laurdan in its sensitivity to the solvent polarity, brightness of TPM image, and precise reflection of the cell environment.[8] The major drawback of the polarity probes such as CL is that their function relies on the generalized polarization (GP) value, which may lead to a significant error due to the ambiguity in determining the range of emission band and the calculation of the G factor.[8,9] A solution to this problem would be to design a turn-on probe that emits TP excited fluorescence (TPEF) exclusively in the domains of lipid rafts.

To address the above needs, we have designed 6-[(*E*)-3-oxo-1-dodecenyl]-2-[*N*-methyl-*N*-(carboxymethyl)amino]naphthalene (CL2) possessing longer conjugation length to enhance the TP cross section for a brighter TPM image and to increase the sensitivity of the fluorescence intensity relative to its environment polarity for the selective detection of the lipid rafts in live cells and tissues without invoking the GP values (Figure 1).

The preparation of CL2 is given in the Supporting Information. The solubility of CL2 in water was 4 $\mu$M, which is sufficient to stain the cells (Figure S2 in the Supporting Information). The spectral data of CL2 are found to be more sensitive to the solvent polarity than CL, as indicated by the larger $\lambda_{max}$ and $\lambda_{max}^{fl}$ values as well as enhanced solvatochromic shifts (Figure S1 and Table S1 in the Supporting Information).[8] Moreover, the fluorescence quantum yield decreased dramatically with the solvent polarity. The fluorescence intensity of CL2 in the vesicles show similar decrease with the hydrophilicity of the liposome in the order 1,2-dipalmitoyl-*sn*-glycero-3-phosphocholine (DPPC) > DOPC/sphingomyelin/cholesterol (1:1:1, raft mixture) > 1,2-dioleoyl-*sn*-glycero-3-phosphocholine (DOPC) (Figure S3 in the Supporting Information). The relative fluorescence intensities of CL2 in DPPC/raft mixture/DOPC in the 410−530 nm range are 8.4/7.4/1.0, respectively. A similar result was observed in the raft mixture with the temperature increase (Figure S4 in the Supporting Information). Hence, the slightly weaker fluorescence in the raft mixture than in DPPC could be explained if CL2 exists in 86/14 ratio in the $l_o/l_d$ domains with the same intensity ratio as in DPPC/DOPC (8.4/1.0). The higher preference of CL2 to reside in the $l_o$ domain can be attributed to its more favorable hydrophobic interactions with sphingomyelin when compared to DOPC.

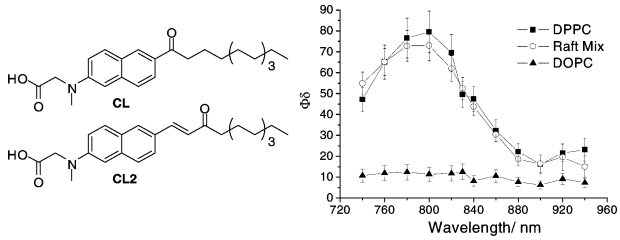


***Figure 1.*** (Left) Structures of CL and CL2. (Right) Two-photon action spectra of CL2 in DPPC (■), raft mixture (○), and DOPC (▲) (lipid/CL2 = 50/1). These data were measured at 25 ± 0.5 °C.

The time-resolved fluorescence (TRF) reveals that CL2 emits from the locally excited (LE) state in DPPC and raft mixture, whereas it emits from both LE and intramolecular charge transfer (ICT) states to give rise to 490 and 572 nm bands in DOPC (Figure S6 and Table S2 in the Supporting Information).[8,10] The fluorescence lifetime of the CL2 is shorter in DOPC (1.4−1.5 ns) than in DPPC (2.7−3.2 ns). Hence, the oscillator strength of the ICT state should be smaller by a factor of ∼5 than that of the LE state to account for the much weaker fluorescence intensity in DOPC. In cells, the TRFs are very similar to those in the raft mixture (Table S2 in the Supporting Information). Thus, the fluorescence of CL2 can discriminate the gel phase (lipid rafts) from the fluid phase because of the combined effects of the preference for the gel phase and the much weaker fluorescence intensity of CL2 in the polar environments.

The TP cross section of CL2 is 250 GM in EtOH (Table S1 in the Supporting Information), which is significantly larger than that of CL (150 GM).[8] This can be attributed to the longer conjugation length. The TP excitation spectra reveal that the two photon action cross section ($\Phi\delta_{max}$) value of CL2 is 8-fold larger in DPPC than in DOPC (Figure 1), which can be attributed to the more hydrophobic environment of DPPC and strong preference of CL2

[†] Department of Chemistry, Korea University.
[‡] National Creative Research Initiative Center for Cell Dynamics, Korea University.
[§] Department of Physics, Korea University.
[||] Biomicrosystems Technology Program, Korea University.
[⊥] Department of Chemistry, Pohang University of Science and Technology.


**10.1021/ja711391f CCC: $40.75** 

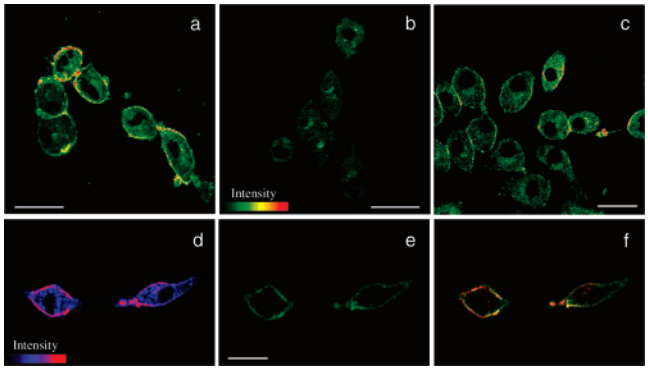


***Figure 2.*** (a−c) Pseudo colored TPM images of CL2-labeled (2 $\mu$M) macrophages before (a) and after (b) treatment with 10 mM M$\beta$CD for 30 min at 37 °C. (c) TPM image of cholesterol depleted macrophages after repletion with 50 $\mu$M cholesterol for 1 h at 37 °C. The cells were labeled with 2 $\mu$M CL2. (d) The domains with high two-photon fluorescence intensity on macrophages labeled with CL2, (e) fluorescence image in the macrophages labeled with BODIPY-$G_{M1}$ and (f) merged image. Excitation wavelengths are 800 nm (a−d) and 488 nm (e), respectively. Scale bars, 30 $\mu$m.

to reside in the $l_o$ domain (vide supra). This allows direct visualization of the $l_o$ domain against the dim background due to the $l_d$ domain by TPM. Furthermore, CL2 showed much higher photostability in DPPC than in DOPC, and visualizing the lipid rafts for a long period of time is feasible (Figure S7 in the Supporting Information).

The TPM images of the CL2-labeled giant unilamellar vesicles (GUVs) composed of DPPC, raft mixture, or DOPC obtained by excitation with horizontally polarized light at 800 nm reveal weakly fluorescent areas in perpendicular direction (Figure S8 in the Supporting Information). This indicates a photoselection effect, that is, CL2 is aligned parallel to the lipid molecules in the membrane probably due to the favorable hydrophilic interactions between the carboxylates and the water molecules near the lipid head groups.[8] A similar result was reported for CL.[8]

To test whether CL2 can visualize the lipid rafts in the model membrane, TPM images of the CL2-labeled GUVs composed of raft mixture were obtained (Figure S9 in the Supporting Information). They reveal intense and dim domains that can be attributed to the existence of discrete $l_o$ and $l_d$ domains (vide supra). Moreover, the TPEF intensity became weaker above the transition temperature (40 °C) and returned to the original level upon cooling, like in the one-photon experiment (Figure S4 in the Supporting Information).

Ⓦ In addition, Movie S1 (in AVI format, see online HTML version) reveals that the $l_o$ domain is floating in the sea of the $l_d$ phase without altering the relative proportions, as predicted by the lipid rafts hypothesis.

Hence, CL2 is clearly capable of detecting the lipid rafts in the model membrane.

CL2 was then tested for detecting the lipid rafts in the live cells. TPM image of CL2-labeled macrophages showed bright regions (red color), which disappeared upon treatment with M$\beta$CD, a lipid raft-destroying reagent (Figure 2a and b), and returned to nearly normal level upon treatment with cholesterol (Figure 2c).[11] To determine unambiguously whether the red-colored domains are indeed the lipid-rafts, the macrophages were co-stained with CL2 and BODIPY-$G_{M1}$, a well-known one-photon fluorescence probe for the lipid raft,[12] and TPM image was co-localized with the one-photon fluorescence image (Figure 2d and e). Bright regions on the two images were well overlapped, confirming that the bright regions reflect lipid rafts (Figure 2f).

To demonstrate the utility of this probe in tissue imaging, acute hippocampal slices from postnatal 3-day mice were incubated with

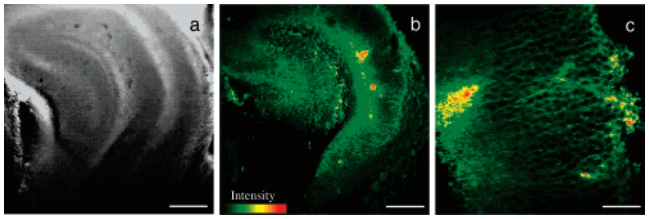


***Figure 3.*** Images of an acute rat hippocampal slice stained with 10 $\mu$M CL2. (a) Bright-field image of the CA1 and CA3 regions as well as the dentate gyrus by 10× magnification. (b) TPM image of the CA1 and CA3 regions by 10× magnification. Twenty-five TPM images were accumulated along the z-direction at the depth of ∼100−250 $\mu$m. (c) TPM image of the CA1 layer at a depth of ∼120 $\mu$m by 40× magnification. The TPM images were collected at 410−530 nm upon excitation at 800 nm with fs pulses. Scale bars, 300 (a,b) and 75 (c) $\mu$m, respectively.

10 $\mu$M CL2 for 30 min at 37 °C. The bright field image of a part of acute mouse hippocampal slice reveals the CA1 and CA3 regions as well as the dentate gyrus (Figure 3a). The TPM images revealed the lipid rafts in the same region at 100−250 $\mu$m depth (Figure S10 in the Supporting Information), but each one represents the distribution exclusively in the given plane. Because the structure of the brain tissue is known to be nonhomogeneous in its entire depth, we have accumulated 25 TPM images obtained at different depth in the range of 100−250 $\mu$m to visualize the distribution of the lipid rafts. The accumulated TPM images show that the lipid rafts are more abundant in the radiatum layer composed of axon bundles than in the pyramidal neuron layer composed of cell bodies (Figure 3b). Moreover, the images taken at higher magnifications resolved the distribution of lipid rafts in the pyramidal neuron layer of the CA1 region (Figure 3c).

To conclude, we have developed a new TP turn-on probe for the lipid rafts. This probe emits much brighter TPEF in lipid rafts than in nonraft domains and allows direct visualization of the lipid rafts in the live cells and pyramidal neuron layer of the CA1 region at a depth of 100−250 $\mu$m in live tissues using TPM.

**Acknowledgment.** This work was supported by a KOSEF grant funded by MOST (R0A-2007-000-20027-0). J.H.H. and K.J.L. were supported by Creative Research Initiatives of the MOST. S.-C.H. was supported by a KOSEF grant (R01-2005-000-10477-0) and the Seoul R&BD program, and J.Y.H. was supported by KRF 2005-070-C00054. T.J. acknowledges the support by the POSTECH core research area program.

**Supporting Information Available:** Synthesis and photophysical properties of CL2, cell culture, two-photon imaging. This material is available free of charge via the Internet at http://pubs.acs.org.

## References

(1) Simons, K.; Toomre, D. *Nat. Rev. Mol. Cell Biol.* **2000**, *1*, 31−39.
(2) Munro, S. *Cell* **2003**, *115*, 377−388.
(3) Anderson, R. G. W.; Jacobson, K. *Science* **2002**, *296*, 1821−1825.
(4) Dykstra, M.; Cherukuri, A.; Sohn, H. W.; Tzeng, S. J.; Pierce, S. K. *Annu. Rev. Immunol.* **2003**, *21*, 457−481.
(5) Mukherjee, S.; Maxfield, F. R. *Annu. Rev. Cell Dev. Biol.* **2004**, *20*, 839−866.
(6) Zipfel, W. R.; Williams, R. M.; Webb, W. W. *Nat. Biotechnol.* **2003**, *21*, 1369−1377.
(7) Helmchen, F.; Denk, W. *Nat. Methods* **2005**, *2*, 932−940.
(8) Kim, H. M.; Choo, H.-J.; Jung, S.-Y.; Ko, Y.-G.; Park, W.-H.; Jeon, S.-J.; Kim, C. H.; Joo, T.; Cho, B. R. *ChemBioChem* **2007**, *8*, 553−559.
(9) Gaus, K.; Gratton, E.; Kable, E. P.; Jones, A. S.; Gelissen, I.; Kritharides, L.; Jessup, W. *Proc. Natl. Acad. Sci. U.S.A.* **2003**, *100*, 15554−15559.
(10) Horng, M. L.; Gardecki, J. A.; Papazyan, A.; Maroncelli, M. *J. Phys. Chem.* **1995**, *99*, 17311−17337.
(11) Furuchi, T.; Anderson, R. G. W. *J. Biol. Chem.* **1998**, *273*, 21099−21104.
(12) Janes, P. W.; Ley, S. C.; Magee, A. I. *J. Cell. Biol.* **1999**, *147*, 447−461.

JA711391F